ELSEVIER

Biochimica et Biophysica Acta 1599 (2002) 125–133

BIOCHIMICA ET BIOPHYSICA ACTA
BBA

www.bba-direct.com

# Reaction kinetic pathway of the recombinant octaprenyl pyrophosphate synthase from *Thermotoga maritima*: how is it different from that of the mesophilic enzyme

Tun-Hsun Kuo [a], Po-Huang Liang [a,b,*]

[a] *Institute of Biochemical Sciences, National Taiwan University, Taipei 10098, Taiwan*
[b] *Institute of Biological Chemistry, Academia Sinica, Nankang, Taipei 11529, Taiwan*

Received 11 April 2002; received in revised form 2 July 2002; accepted 1 August 2002

**Abstract**

Octaprenyl pyrophosphate synthase (OPPs) catalyzes the chain elongation of farnesyl pyrophosphate (FPP) via consecutive condensation reactions with five molecules of isopentenyl pyrophosphate (IPP) to generate all-*trans* $C_{40}$-octaprenyl pyrophosphate. The polymer forms the side chain of ubiquinone that is involved in electron transport system to produce ATP. Our previous study has demonstrated that *Escherichia coli* OPPs catalyzes IPP condensation with a rate of 2 $s^{-1}$ but product release limits the steady-state rate at 0.02 $s^{-1}$ [Biochim. Biophys. Acta 1594 (2002) 64]. In the present studies, a putative gene encoding for OPPs from *Thermotoga maritima*, an anaerobic and thermophilic bacterium, was expressed, purified, and its kinetic pathway was determined. The enzyme activity at 25 °C was 0.005 $s^{-1}$ under steady-state condition and was exponentially increased with elevated temperature. In contrast to *E. coli* OPPs, IPP condensation rather than product release was rate limiting in enzyme reaction. The product of chain elongation catalyzed by *T. maritima* OPPs was $C_{40}$ and the rate of its conversion to $C_{45}$ was negligible. Under single-turnover condition with 10 μM OPPs·FPP complex and 1 μM IPP, only the $C_{20}$ was formed rather than $C_{20}$–$C_{40}$ observed for *E. coli* enzyme. Together, our data suggest that the thermophilic OPPs from *T. maritima* has lower enzyme activity at 25 °C, higher product specificity, higher thermal stability and lower structural flexibility than its mesophilic counterpart from *E. coli*.


*Keywords:* Prenyltransferase; Ubiquinone; Single-turnover; Thermophile; Mesophile

## 1. Introduction

Thermophiles are organisms that can grow under high temperature conditions (>50 °C). Proteins in thermophiles are heat resistant and maintain proper three-dimensional structure even at extremely high temperatures, allowing the organism to survive the harsh environment. However, little is known about how the proteins of a thermophile differ from those of a mesophile to account for their thermostability. Sequence comparisons show that hyperthermophilic and mesophilic versions of the same enzyme typically share about 30–50% identity [1]. Even the crystal structure for a hyperthermophilic rubredoxin containing only 53 amino acids from the archaebacterium *Pyrococcus furiosus* shows that it is virtually superimposable on its mesophilic counterpart [2]. The relatively minor changes in protein structure apparently enhance packing via additional interactions such as salt bridges and hydrogen bonds.

In this study, a putative octaprenyl pyrophosphate synthase (OPPs) identified from *Thermotoga maritima* genome by sequence comparison (Fig. 1) was chosen as the model system to examine the activity, product specificity, thermal stability and structural flexibility of the enzyme in comparison with its mesophilic counterpart from *Escherichia coli*. *T. maritima* was originally isolated from geothermal heated marine sediment at Vulcano, Italy. This organism is an

*Abbreviations:* OPPs, octaprenyl pyrophosphate synthase; OPP, octaprenyl pyrophosphate; FPP, farnesyl pyrophosphate; IPP, isopentenyl pyrophosphate; PCR, polymerase chain reaction; IPTG, isopropyl-β-D-thiogalactopyranoside; Ni-NTA, nickel nitrilo-tri-acetic acid; Tris, tris(hydroxymethyl)aminomethane; Hepes, 4-(2-hydroxyethyl)-1-piperazineethanesulfonic acid; EDTA, ethylenediaminetetraacetic acid; SDS-PAGE, sodium dodecyl sulfate-polyacrylamide gel electrophoresis; TLC, thin layer chromatography; MW, molecular weight

* Corresponding author. Institute of Biological Chemistry, Academia Sinica, Nankang, Taipei 11529, Taiwan. Tel.: +886-2-2785-5696x6070; fax: +886-2-2788-9759.

*E-mail address:* phliang@gate.sinica.edu.tw (P.-H. Liang).

1570-9639/02/$ - see front matter © 2002 Elsevier Science B.V. All rights reserved.
PII: S1570-9639(02)00410-7


Fig. 1. Alignment of *T. maritima* OPPs (TC40) sequence with that of *E. coli* OPPs (C40), *Synechocystis* sp. solanesyl pyrophosphate synthase (C45) and *M. tuberculosis* heptaprenyl pyrophosphate synthase (C35). Black and gray outlines indicate identical and similar amino acid residues, respectively.

anaerobic bacterium and has optimum growth temperature of 80 °C [3]. OPPs belongs to a prenyltransferase family that catalyzes the chain elongation of allylic pyrophosphate via condensation with IPP [4,5]. As shown in Scheme 1, the enzyme catalyzes the condensation reactions of farnesyl pyrophosphate (FPP) with five molecules of isopentenyl pyrophosphate (IPP) to produce $C_{40}$ octaprenyl pyrophosphate (OPP) [6,7]. OPPs is responsible for the biosynthesis of ubiquinone side chain in *E. coli* [8,9]. Other organisms contain ubiquinone with designate lengths of side chain synthesized by specific prenyltrasnferases [10]. For example, the lengths of ubiquinone side chain are $C_{30}$ for yeast *S. cerevisiae*, $C_{45}$ for rat and $C_{50}$ for human, which are synthesized by hexaprenyl pyrophosphate synthase, solanesyl pyrophosphate synthase and decaprenyl pyrophosphate synthase, respectively [11–13]. We had studied the OPPs in *E. coli* and found that the enzyme generated products longer than $C_{40}$ [14]. However, the rate constant (0.02 $s^{-1}$) for formation of the product with additional IPP condensation is 100-fold smaller than that (2 $s^{-1}$) for $C_{40}$ production. Moreover, under the condition with *E. coli* OPPs·FPP (10 μM) in much excess of IPP (1 μM), $C_{20}$–$C_{40}$ rather than $C_{20}$ alone were generated [14]. This may be due to a higher IPP affinity of OPPs·intermediate relative to OPPs·FPP, a property reflecting the flexible protein conformation [15]. We report in this paper the characterization of a recombinant OPPs from *T. maritima* focusing on its reaction kinetics, product specificity, thermal stability and structural flexibility.

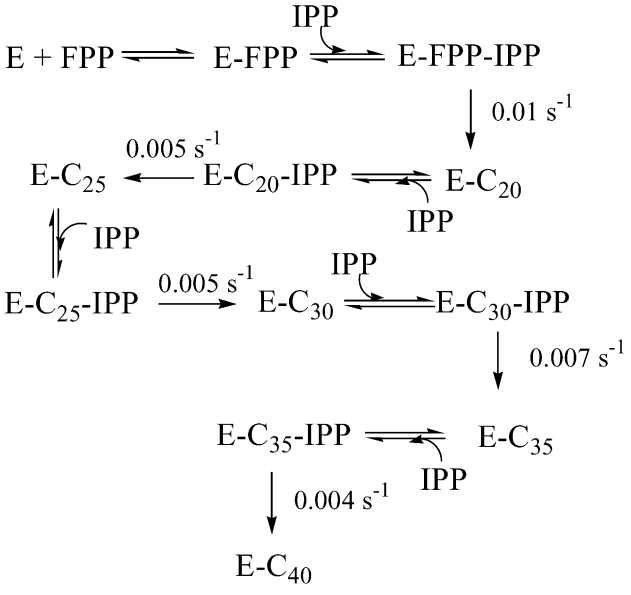


Scheme 1. The kinetic scheme proposed for *T. maritima* OPPs reaction.

## 2. Materials and methods

### 2.1. Chemicals

[$^{14}$C]IPP (55 mCi/mmol) radiolabeled substrate was purchased from Amersham Pharmacia Biotech and FPP was product of Sigma Co. Reverse phase TLC for product analysis was obtained from Merck (Darmstadt, Germany). The plasmid mini-prep kit, DNA gel extraction kit and Ni-NTA were the products of QIAGEN. Potato acidic phosphatase (2 Unit/mg) was purchased from Boehringer Mannheim. The pET-32Xa/LIC vector, competent cells *E. coli* JM109 and BL21 (DE3), T4 DNA polymerase, and Factor Xa were obtained from Novagen. All other buffer and reagents were of the highest commercial purity. Millipore ultrapure $H_2O$ was used in all experiments.

### 2.2. Overexpression of OPPs from T. maritima

*T. maritima* obtained from American type culture collection (ATCC) was grown at 80 °C under anaerobic con-

dition in the medium prepared according to protocol provided by ATCC. The genomic DNA was obtained from the harvested cells using DNA extraction kit according to manufacturer's instruction. Using its genomic DNAs as template, the gene encoding OPPs from the bacterium was amplified by carrying out polymerase chain reaction (PCR). The forward primer 5′ ATGACGAAAAACAAGCTGAACCAA 3′ and reverse primer 5′ TCATGAAGAGATTTTGATTTTAAA 3′ were utilized in the PCR. The PCR product (OPPs gene) was purified from 0.8% agarose gel electrophoresis and used as a template for the second PCR to create FXa cleavage site and the complementary sequences for the vector pET-32Xa/LIC. In this PCR reaction, the forward primer 5′ GGTATTGAGGGTCGCATGACGAAAAACAAG 3′ and the reverse primer 5′ AGAGGAGAGTTAGAGCCTCATGAAGAGATT 3′ were employed. The DNA product was ligation with the vector and transformed into *E. coli* BL21 (DE-3) for protein expression as previously described [14].

### 2.3. Purification of recombinant T. maritima OPPs

The purification procedure of recombinant *T. maritima* OPPs was the same as previously reported for *E. coli* OPPs [14]. The cell lysate was loaded onto a Ni-NTA column and the protein with His tag was finally eluted with 25 mM Tris (pH 7.5), 150 mM NaCl and 300 mM imidazole. The protein solution was dialyzed twice against 2 l buffer (25 mM Tris, pH 7.5, and 150 mM NaCl) and digested with FXa to remove tag. The untagged protein was separated from the tag by loading onto a Ni-NTA column. The tag was bound to Ni-NTA and the OPPs eluted by a buffer of 25 mM Tris, pH 7.5, 5 mM imidazole and 150 mM NaCl was highly pure according to SDS-PAGE analysis.

### 2.4. Steady-state $K_m$ and $k_{cat}$ measurements

The OPPs reaction was initiated by adding 0.1 μM enzyme (final concentration) to a mixture containing various concentrations of FPP (1–10 μM) and [$^{14}$C]IPP (1–50 μM) in 100 mM Hepes buffer (pH 7.5), 50 mM KCl and 0.5 mM $MgCl_2$ at 25 °C. The enzyme concentration used in all experiments was determined from its absorbance at 280 nm (extinction coefficient=20340 $M^{-1}$ $cm^{-1}$). Within 10% substrate depletion, the reaction mixture was periodically withdrawn. The reaction was terminated by adding 10 mM (final concentration) EDTA and the product was extracted with 1-butanol. The product was quantitated by counting the radioactivity in butanol phase ([$^{14}$C]IPP was in aqueous phase) using a Beckmann LS6500 scintillation counter. The OPPs steady-state $k_{cat}$ was calculated based on the rate of IPP consumption. The initial rate was calculated by plotting the [IPP] consumed versus time and the kinetic constants were obtained by fitting the data with the Michaelis–Menten equation using KaleidaGraph computer software (synergy software).

### 2.5. Temperature dependence of OPPs activity

The activity was measured as described above in a reaction mixture containing 0.1 μM OPPs, 5 μM FPP, 50 μM [$^{14}$C]IPP in a buffer of 100 mM Hepes (pH 7.5), 0.5 mM $MgCl_2$ and 50 mM KCl at temperature ranging from 25 to 85 °C. The enzyme was added to a pre-heated mixture to initiate the reaction. The initial rate in the first 5 min of reaction was measured at each temperature.

### 2.6. Single-turnover experiments

The single-turnover reaction was initiated by mixing 15 μl of the enzyme (10 μM) preincubated with FPP (2 μM) with equal volume of [$^{14}$C]IPP (50 μM) solution in buffer containing 100 mM Hepes (pH 7.5), 0.5 mM $MgCl_2$ and 50 mM KCl at 25 °C. The concentrations cited in the parentheses and hereafter in the paper are those after mixing. The reaction mixture quenched with EDTA in specified time period was extracted with the same volume of 1-butanol and the radioactivity in the organic phase (intermediates and product) was counted by the scintillation counter (Beckmann LS6500). For identification of intermediates and product at each time point, the radiolabeled polyprenyl pyrophosphates were extracted with 1-butanol and treated with 20% propanol, 4.4 U/ml acidic phosphatase, 0.1% Triton X-100 and 50 mM sodium acetate (pH 4.7) to be converted to the corresponding polyprenols [16]. The products were separated by reverse phase TLC with acetone/water (19:1) as mobile phase and the product distribution was determined by autoradiography [17]. The time course for each intermediate was simulated by KINSIM computer program as described below.

### 2.7. Data simulation

The KINSIM program [18] simulation of the kinetic data presented in this paper is as described in our previous report [14]. The derived kinetic pathway of the *T. maritima* OPPs reaction is shown in Scheme 1 and the details of the kinetic simulation of the data are shown in Chart 1.

### 2.8. OPPs molecular weight determination

The molecular weight of the recombinant OPPs was determined by size-exclusion chromatography on a Blue Dextran 2000 calibrated pre-packed Sephadex G-200 column (1×20 cm, Amsheram Pharmacia Biotech). The molecular weight was estimated from the plot of $K_{av}$ vs. log MW of protein molecular weight standards, which were catalase (206,000), aldolase (170,000), bovine serum

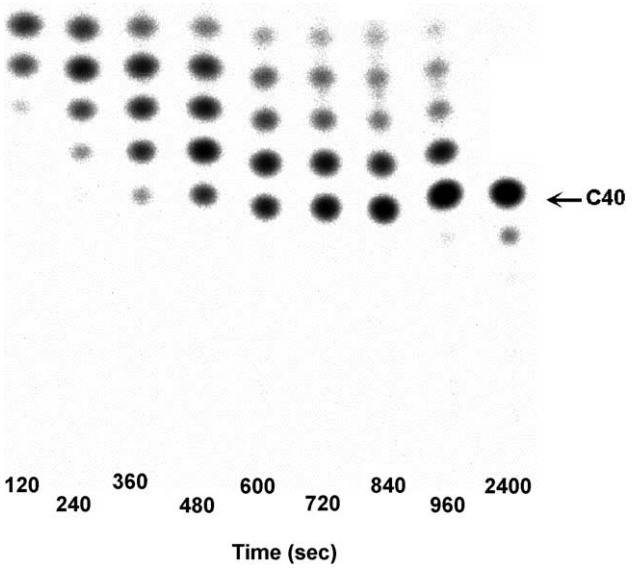


Plate 1. The intermediates and product formed during the *T. maritima* OPPs single-turnover reaction with 10 mM enzyme, 2 mM FPP and 50 mM [$^{14}$C]IPP at pH 7.5 and 25 °C. The reaction continued for 120 to 960 s and an extended period of 2400 s.

albumin (67,000), and ovalbumin (43,000). A buffer containing 25 mM Tris (pH 7.5) and 150 mM NaCl was used to elute the proteins at a flow rate of 0.5 ml/min. The $K_{av}$ values were calculated using the equation $K_{av}=(V_e-V_o)/(V_t-V_o)$ where $V_e$ is elution volume of the protein, $V_o$ is the elution volume of Blue Dextran 2000 and $V_t$ is total gel bed volume [19].

### 2.9. Circular dichroism (CD) experiments

For determination of secondary structure of *T. maritima* and *E. coli* OPPs enzymes, CD measurements were made on a Jasco J-710 spectrophotometer in a 0.1 cm water-jacketed cuvette. The ellipticity of 200-μl sample containing 1 μM OPPs in a buffer of 25 mM Tris (pH 7.5) and 150 mM NaF 25 °C was recorded from 200 to 260 nm. Spectra reported were the average of three scans collected at 30 nm/min with a 2-s response time. The secondary structure of the protein was analyzed using the program SELCON2 [20]. For the measurement of thermal stability, the ellipticity of 10 μM enzyme was monitored at 208 nm and the temperature was increased at a rate of 30 °C/h. Thermal unfolding curve of *E. coli* OPPs was fitted with a two-state unfolding model [21].

### 2.10. Final product distribution

The reaction mixture containing different concentrations of OPPs, [$^{14}$C]IPP and FPP in buffer of 100 mM Hepes buffer (pH 7.5), 0.5 mM $MgCl_2$ and 50 mM KCl, was incubated at 25 °C for 100 h. The reaction was terminated with 10 mM EDTA. We then extracted the products with 1-butanol, evaporated the solvent under $N_2$, converted the products to polyprenols and analyzed the polyprenols by TLC as described above.

## 3. Results

### 3.1. Temperature dependence of the *T. maritima* OPPs activity and the $T_m$ value

The $k_{cat}$ value of recombinant OPPs of *T. maritima* is 0.005 $s^{-1}$ and FPP and IPP $K_m$ values are 1.5 and 2 μM, respectively, at 25 °C and pH 7.5. The enzyme activities at temperatures ranging from 25 to 85 °C exponentially increased with elevated temperature (Fig. 2A). According to Arrhenius equation, the activation energy ($E_a$) required for the reaction is calculated to be 16.2 kcal/mol. Measured by CD spectrophotometer, the temperature at which *T. maritima* OPPs is half-folded ($T_m$) is >80 °C, higher than that of *E. coli* enzyme (55.3 °C), indicating that *T. maritima* OPPs has higher thermal stability (Fig. 2B).

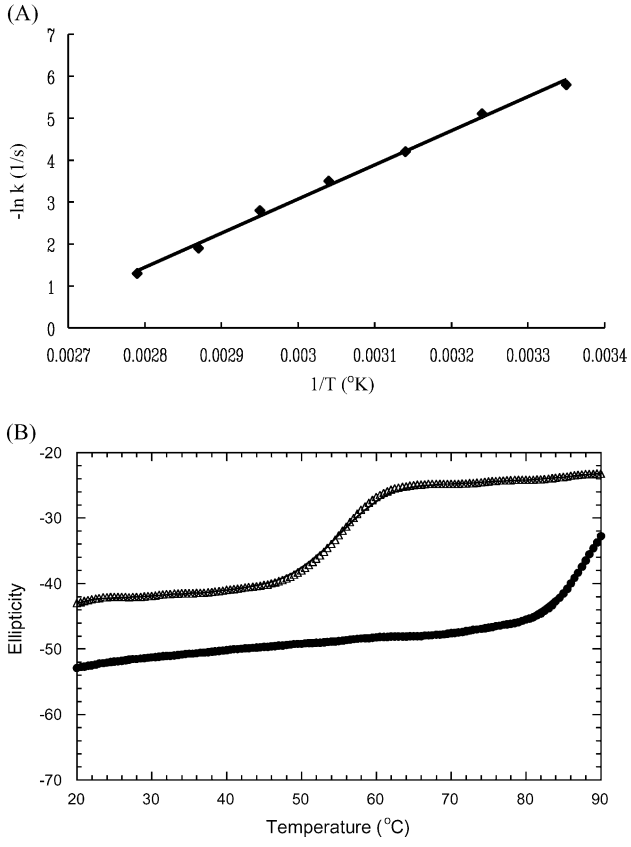


Fig. 2. (A) *T. maritima* OPPs activity measured at different temperature. The initial rate in the first 5 min of the enzyme reaction of 0.1 μM enzyme with 5 μM FPP and 50 μM [$^{14}$C]IPP was measured at temperature ranging from 25 to 85 °C. (B) Thermal stabilities of recombinant OPPs from *E. coli* and *T. maritima* monitored by CD. The ellipticity at 208 nm was monitored from 25 to 90 °C using 10 μM *E. coli* OPPs (△) and 10 μM *T. maritima* enzyme (●) The half-folded $T_m$ was 55.3 °C for *E. coli* enzyme by fitting the data with a two-state unfolding model. For *T. maritima* OPPs, the unfolding was not completed at 90 °C.

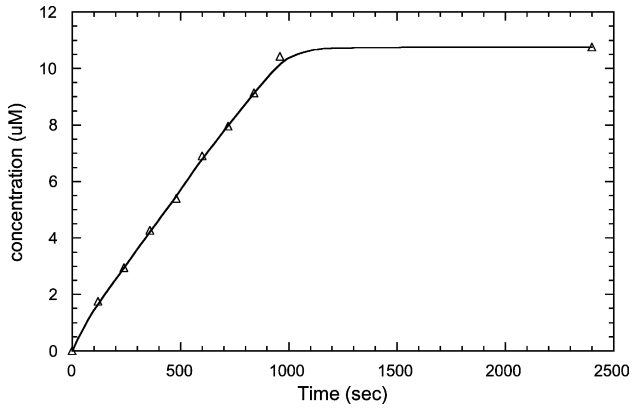


Fig. 3. The single-turnover reaction of *T. maritima* OPPs with enzyme in excess of FPP. A solution containing enzyme (10 μM) preincubated with FPP (2 μM) was mixed with [$^{14}$C]IPP (50 μM) at pH 7.5 and 25 °C. The products of IPP condensation formed at each time point were quantitated by scintillation counting of the radioactivity in the butanol layer. The curve represents a fit by KINSIM simulation using rate constants shown in Scheme 1.

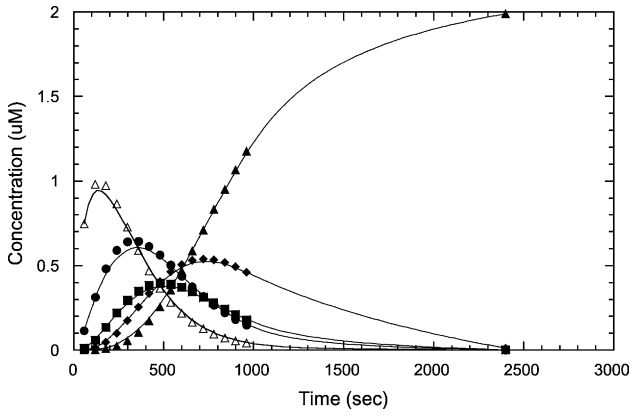


Fig. 4. Single-turnover time courses of intermediates ($C_{20}$–$C_{35}$) and product ($C_{40}$) in OPPs reaction. *T. maritima* OPPs enzyme (10 μM) preincubated with FPP (2 μM) was mixed with [$^{14}$C]IPP (50 μM) at pH 7.5 and 25 °C. The data represent the time courses of $C_{20}$ (△), $C_{25}$ (●), $C_{30}$ (■), $C_{35}$ (♦) and $C_{40}$ (▲). The fitting curves were obtained from KINSIM simulation using the kinetic pathway shown in Scheme 1.

### 3.2. Complete kinetic pathway of T. maritima OPPs

Due to the great hydrophobicity of the product, the reaction rates of the long-chain polyprenyl synthetic enzymes are often limited by slow product release under steady-state condition [14,22,23]. The 3-D structure of the $C_{55}$-undecaprenyl pyrophosphate synthase implicates the strong hydrophobic interactions between the enzyme and the product and provides a rationale for the slow product release [24]. In order to measure the IPP condensation rate constant, we have to perform the single-turnover experiments with higher enzyme concentration than the substrate FPP so that product release is not limiting the reaction rate [14,22,23]. The formation of $C_{20}$–$C_{40}$ catalyzed by *T. maritima* OPPs was examined during the enzyme single-turnover reaction containing 10 μM enzyme, 2 μM FPP and 50 μM [$^{14}$C]IPP. The total formation of radiolabeled species with time in the reaction is shown in Fig. 3. Since the percentages of $C_{20}$–$C_{40}$ at each time point of the reaction were obtained by imaging as shown in Plate 1, the time courses of these intermediates could be determined (Fig. 4). The data were fitted using KINSIM program to obtain rate constant for individual IPP condensation catalyzed by OPPs. The derived kinetic pathway of *T. maritima* OPPs reaction is summarized in Scheme 1. The fit of the total IPP incorpo-

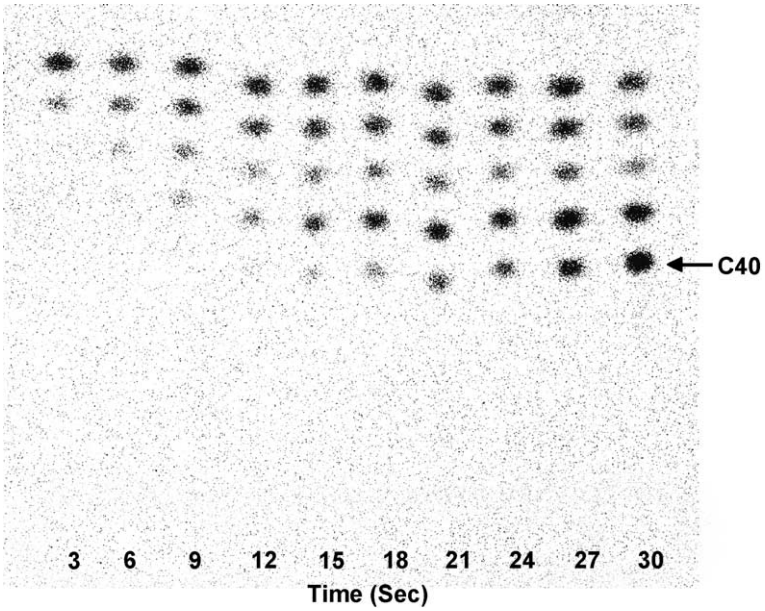


Plate 2. The intermediates and product formed during the *T. maritima* OPPs single-turnover reaction with 10 mM enzyme, 2 mM FPP and 50 mM [$^{14}$C]IPP at pH 7.5 and 80 °C. The reaction time was from 3 to 30 s. The $C_{40}$ product was formed much earlier than the same reaction performed at 25 °C.

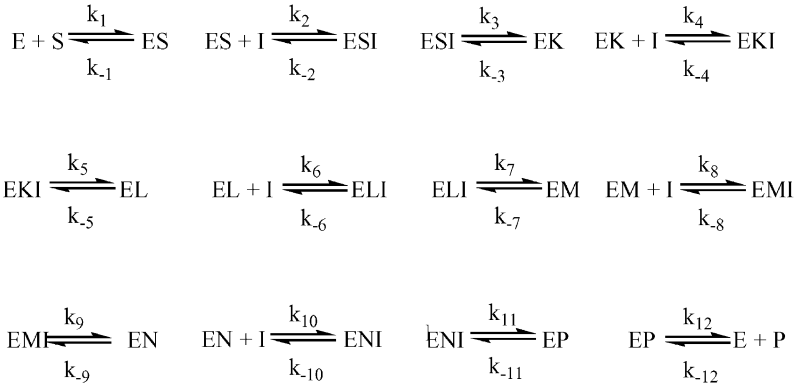


E = enzyme; I = IPP; S = $C_{15}$-FPP; K = $C_{20}$; L = $C_{25}$; M = $C_{30}$; N = $C_{35}$; P = $C_{40}$;

*Rate constants*

$k_1 = 10\ \mu M^{-1}\ s^{-1}$ $k_{-1} = 15\ s^{-1}$ $k_2 = 10\ \mu M^{-1}\ s^{-1}$ $k_{-2} = 20\ s^{-1}$ $k_3 = 0.01\ s^{-1}$ $k_{-3} = 0\ s^{-1}$
$k_4 = 10\ \mu M^{-1}\ s^{-1}$ $k_{-4} = 20\ s^{-1}$ $k_5 = 0.005\ s^{-1}$ $k_{-5} = 0\ s^{-1}$ $k_6 = 10\ \mu M^{-1}\ s^{-1}$ $k_{-6} = 20\ s^{-1}$
$k_7 = 0.005\ s^{-1}$ $k_{-7} = 0\ s^{-1}$ $k_8 = 10\ \mu M^{-1}\ s^{-1}$ $k_{-8} = 20\ s^{-1}$ $k_9 = 0.007\ s^{-1}$ $k_{-9} = 0\ s^{-1}$
$k_{10} = 10\ \mu M^{-1}\ s^{-1}$ $k_{-10} = 20\ s^{-1}$ $k_{11} = 0.004\ s^{-1}$ $k_{-11} = 0\ s^{-1}$ $k_{12} = 15\ s^{-1}$ $k_{-12} = 10\ \mu M^{-1}\ s^{-1}$

Chart 1. Kinetic constants used to simulate the time course of *T. maritime* OPPs single-turnover reaction.

ration with time during the single-turnover reaction (Fig. 3) is obtained by using these kinetic constants to sum up all the intermediates in each specified time period of reaction. As shown in Scheme 1, the rate constant determined for each of the five IPP condensation steps leading to $C_{40}$ product formation is approximately the same ($\sim 0.005\ s^{-1}$) according to KINSIM simulation. Because this rate constant equals to the steady-state $k_{cat}$ value, the IPP condensation represents the rate-limiting step of the *T. maritima* OPPs reaction. In contrast, the IPP condensation rate constant (2 $s^{-1}$) of *E. coli* OPPs is $10^3$ times larger at 25 °C. However, at 80 °C, the *T. maritima* OPPs activity is greatly enhanced (Plate 2), consistent with the predicted increase of IPP condensation rate. This indicates that at high temperature, the IPP condensation is still a rate-limiting step for *T. maritima* enzyme.

### 3.3. Composition and secondary structure of T. maritima OPPs

In order to search for the possible cause of the significant reduction of OPPs activity at room temperature, we performed gel filtration chromatography to determine the composition of *T. maritima* OPPs and found that the enzyme is a dimer (data not shown). *E. coli* OPPs also is a dimeric enzyme and its dimerization is essential for product chain length determination [25]. Furthermore, the secondary structure of *T. maritima* OPPs measured using CD spectrophotometer is compared to that of *E. coli* enzyme. As shown in Fig. 5, both CD spectra are similar with the α helix and β sheet contents of 52% and 23% for *E. coli* OPPs, and 59% and 26% for *T. maritima* OPPs, respectively, indicating the similar secondary structure for the two enzymes.

### 3.4. Product distribution of OPPs reaction

From the data presented above, under single-turnover condition $C_{40}$ is the exclusive product of *T. maritima* OPPs reaction. We had further examined the enzyme final prod-

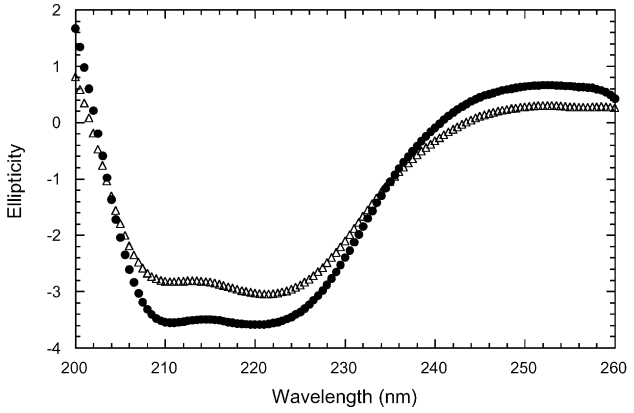


Fig. 5. Analysis of secondary structures of *T. maritima* and *E. coli* OPPs enzymes using CD. The ellipticities of 1 μM *E. coli* enzyme (△) and 1 μM *T. maritima* enzyme (●) were recorded from 200 to 260 nm. Two enzymes have similar secondary structure according to their CD spectra.

ucts after a long-time incubation (100 h) under a variety of different conditions. The results are shown in Fig. 6 and the quantitative data are summarized in Table 1. As shown in lane 1 of the figure, under multiple turnovers with 0.2 μM enzyme, 50 μM [$^{14}$C]IPP and 50 μM FPP, the $C_{20}$–$C_{40}$ products were formed. This is due to that the IPP condensation rate is slow (~0.005 $s^{-1}$) and FPP has a chance to displace the intermediates from the active site. Under the increased ratio of IPP to FPP (FPP concentration was reduced to 5 μM) as shown in lane 2, $C_{40}$ and very small amount of $C_{45}$ were generated. The rate of $C_{40}$ conversion to $C_{45}$ was extremely slow ($2\times10^{-5}$ $s^{-1}$). No further elongated product larger than $C_{45}$ could be observed even at high temperature 80 °C where OPPs has enhanced activity (data not shown). An OPPs reaction with [E·FPP]>[IPP] was performed to monitor the product formation with limited amount of IPP. The reaction shown in lane 3 of the figure contained 10 μM thermophilic OPPs, only 1 μM [$^{14}$C]IPP and excessive FPP (50 μM). Under this condition where the E·FPP concentration was 10-fold higher than that of IPP, $C_{20}$-geanylgeranyl pyrophosphate was found as sole product. The result remained the same when the reaction was performed at 80 °C (data not shown). This represents an interesting difference between *T. maritima* OPPs and *E. coli* enzyme since the later generates $C_{20}$–$C_{40}$ as products under the same condition [14]. In a control reaction shown in lane 4, $C_{40}$ was synthesized by 10 μM *T. maritima* enzyme when FPP concentration was reduced to 0.1 μM and [$^{14}$C]IPP concentration remained as 1 μM.

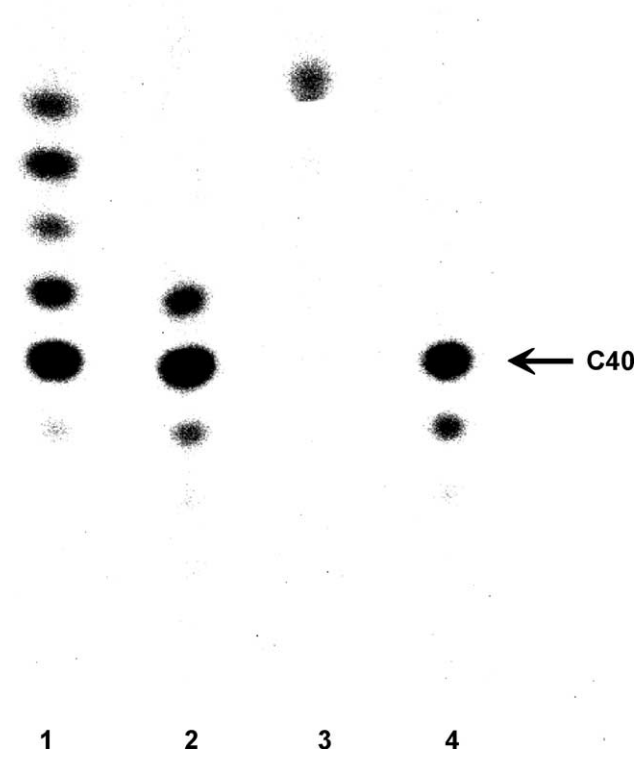


Fig. 6. The product distribution of *T. maritima* OPPs reaction using FPP and [$^{14}$C]IPP as substrates under various conditions for 100 h at 25 °C. The reaction conditions are lane 1: 0.2 μM enzyme with 50 μM [$^{14}$C]IPP and 50 μM FPP; lane 2: 0.2 μM enzyme with 50 μM [$^{14}$C]IPP and 5 μM FPP; lane 3: 10 μM enzyme with 1 μM [$^{14}$C]IPP and 50 μM FPP; lane 4: 10 μM enzyme with 1 μM [$^{14}$C]IPP and 0.1 μM FPP.

Table 1
Product distribution of *T. maritima* OPPs catalyzed condensation reactions of IPP with FPP under various conditions

| Condition | Product (%) | | | | | |
|---|---|---|---|---|---|---|
| | $C_{20}$ | $C_{25}$ | $C_{30}$ | $C_{35}$ | $C_{40}$ | $C_{45}$ |
| 0.2 μM E; 50 μM FPP; 50 μM IPP | 28.0 | 22.3 | 7.6 | 11.9 | 28.3 | 1.8 |
| 0.2 μM E; 5 μM FPP; 50 μM IPP | – | – | – | 20.7 | 72.5 | 6.9 |
| 10 μM E; 50 μM FPP; 1 μM IPP | 100 | – | – | – | – | – |
| 10 μM E; 0.1 μM FPP; 1 μM IPP | – | – | – | – | 87.2 | 12.8 |

## 4. Discussion

The OPPs encoding gene has been identified from the complete genome sequences of *T. maritima* using BLAST program [26]. This gave no firm answer regarding to the chain length of enzyme product as the sequence of *T. maritima* OPPs has 32%, 32% and 31% similarity with that of *E. coli* OPPs, *Synechocystis* sp. $C_{45}$-solanesyl pyrophopshate synthase and *Mycobacterium tuberculosis* $C_{35}$-heptaprenyl pyrophosphate synthase, respectively (Fig. 1). We identify in this study the product of this putative enzyme to be $C_{40}$. In order to know how a thermophilic enzyme is different from the corresponding enzyme in a mesophile (*E. coli*), we conducted experiments to reveal the different properties of two enzymes at 25 °C. The $k_{cat}$ value of the *T. maritima* OPPs reaction measured under steady-state condition is 0.005 $s^{-1}$, consistent with the rate of IPP condensation obtained from enzyme single-turnover experiments. Therefore, the IPP condensation represents the rate-limiting step of the *T. maritima* OPPs reaction. In contrast, the IPP condensation catalyzed by *E. coli* OPPs is 2 $s^{-1}$ and the product release (steady-state rate) is 100-fold slower, indicating that the product release is rate determining. Despite the sequence homology between two enzymes, *T. maritima* OPPs has $10^3$ times lower activity in IPP condensation compared to *E. coli* OPPs at 25 °C. However, with increased temperature, the *T. maritima* enzyme has elevated level of activity. The activity of OPPs in *T. maritima* at high temperature is required for biosynthesis of menaquinone as a putative 1,4-dihydroxy-2-naphthoate octaprenyltransferase is identified in the genome of the bacterium. Indeed, most Gram-positive bacteria and anaerobic Gram-negative bacteria contain only menaquinone [27]. The reason for causing 1000-fold lower activity in *T. maritima* OPPs at 25 °C must be due to a subtle change in the tertiary structure since the composition and secondary structure are similar for two enzymes.

The rate for an extra IPP incorporation into OPP is 0.02 $s^{-1}$ and products with excessive IPP molecules were observed for *E. coli* OPPs [14]. However, for *T. maritima* OPPs, it is almost negligible ($2\times10^{-5}$ $s^{-1}$) for the formation of $C_{45}$ and the larger polymers than $C_{45}$ are not observed even at high temperature where the *T. maritima* enzyme has higher activity. Apparently, *T. maritima* OPPs has higher product specificity compared to *E. coli* OPPs. Moreover, the product under the IPP single-turnover reaction of 10 μM *T. maritima* OPPs·FPP complex with 1 μM IPP is $C_{20}$ geranylgeranyl pyrophosphate at 25 °C and at high temperature (80 °C). In contrast, *E. coli* OPPs produces $C_{20}$–$C_{40}$ compounds under the same condition. The intermediate-bound OPPs from *E. coli* might undergo conformational change to increase its affinity with IPP leading to formation of product at lower concentration of IPP than OPPs·FPP. The undecaprenyl pyrophosphate synthase that shows similar pattern of product distribution has a flexible structure as a protein conformational change was observed during catalysis [28]. However, this unique phenomenon was not seen in *T. maritima* OPPs.

In summary, we have utilized a pre-steady-state method to analyze the complete kinetic pathway of *T. maritima* OPPs reaction, which was not previously determined. This kinetic pathway contains five IPP condensation steps with a rate of ~0.005 $s^{-1}$ for each step simulated from our kinetic data. Despite the similar secondary structure, the enzyme has lower enzyme activity at 25 °C, higher product specificity, higher thermal stability and lower structural flexibility than its mesophilic *E. coli* counterpart.

## Acknowledgements

This study was supported by a grant (NSC91-2113-M-001-007) from National Council of Science of Taiwan and a grant from Academia Sinica.

## References

[1] M.W.W. Adams, Enzymes and proteins from organisms that grow near and above 100 degrees Celsius, Annu. Rev. Microbiol. 47 (1993) 627–658.
[2] M.W. Day, B.T. Hsu, L. Joshua-Tor, J.B. Park, Z.H. Zhou, M.W. Adams, D.C. Rees, X-ray crystal structures of the oxidized and reduced forms of the rubredoxin from the marine hyperthermophilic archaebacterium *Pyrococcus furiosus*, Protein Sci. 1 (1992) 1494–1507.
[3] R. Huber, T.A. Langworthy, H. Konig, M. Thomm, C.R. Woese, U.B. Sleytr, K.O. Stetter, *Thermotoga maritima* sp. nov. represents a new genus of unique extremely thermophilic eubacteria growing up to 90 °C, Arch. Microbiol. 144 (1986) 324–333.
[4] K. Ogura, T. Koyama, H. Sagami, Polyprenyl diphosphate synthases, Sub-cell. Biochem. 28 (1997) 57–87(Chapter 3).
[5] K. Ogura, T. Koyama, Enzymatic aspects of isoprenoid chain elongation, Chem. Rev. 98 (1998) 1263–1276.
[6] S. Fujisaki, T. Nishino, H. Katsuki, Isoprenoid synthesis in *Escherichia coli*. Separation and partial purification of four enzymes involved in the synthesis, J. Biochem. 99 (1986) 1327–1337.
[7] K.-I. Asai, S. Fujisaki, Y. Nishimura, T. Nishino, K. Okada, T. Nakagawa, M. Kawamukai, H. Matsuda, The identification of *Escherichia coli ispB (cel)* gene encoding the octaprenyl diphosphate synthase, Biochem. Biophys. Res. Commun. 202 (1994) 340–345.
[8] K. Okada, K. Suzuki, Y. Kamiya, X. Zhu, S. Fujisaki, Y. Nishimura, T. Nishino, T. Nakagawa, M. Kawamukai, H. Matsuda, Polyprenyl diphosphate synthase essentially defines the length of the side chain of ubiquinone, Biochim. Biophys. Acta 1302 (1996) 217–223.
[9] K. Okada, M. Minehira, X. Zhu, K. Suzuki, T. Nakagawa, H. Matsuda, M. Kawamukai, The *ispB* gene encoding octaprenyl diphosphate synthase is essential for growth of *Escherichia coli*, J. Bacteriol. 179 (1997) 3058–3060.
[10] M.D. Collin, D. Jones, Distribution of isoprenoid quinone structural types in bacteria and their taxonomic implication, Microbiol. Rev. 45 (1981) 316–354.
[11] M.N. Ashby, P.A. Edwards, Elucidation of the deficiency in two yeast coenzyme Q mutants. Characterization of the structural gene encoding hexaprenyl pyrophosphate synthetase, J. Biol. Chem. 265 (1990) 13157–13164.
[12] H. Teclebrhan, J. Olsson, E. Swiezewska, G. Dallner, Biosynthesis of the side chain of ubiquinone:trans-prenyltransferase in rat liver microsomes, J. Biol. Chem. 268 (1993) 23081–23086.
[13] L. Ernster, G. Dallner, Biochemical, physiological and medical aspects of ubiquinone function, Biochim. Biophys. Acta 1271 (1995) 195–204.
[14] J.J. Pan, T.H. Kuo, Y.K. Chen, L.W. Yang, P.H. Liang, Insight into the activation mechanism of *E. coli* octaprenyl pyrophosphate synthase derived from pre-steady-state kinetic analysis, Biochim. Biophys. Acta 1594 (2002) 64–73.
[15] P.H. Liang, T.P. Ko, A.H.-J. Wang, Structure, mechanism and function of prenyltransferases, Eur. J. Biochem. 269 (2002) 3339–3354 (doi:10.1046/j.1432-1033.2002.03014.x).
[16] H. Fujii, T. Koyama, K. Ogura, Efficient enzymatic hydrolysis of polyprenyl pyrophosphate, Biochim. Biophys. Acta 712 (1982) 716–718.
[17] N. Shimizu, T. Koyama, K. Ogura, Molecular cloning, expression, and purification of undecaprenyl diphosphate synthase, J. Biol. Chem. 273 (1998) 19476–19481.
[18] B.A. Barshop, R.F. Wrenn, C. Frieden, Analysis of numerical methods for computer simulation of kinetic processes: development of KINSIM—a flexible, portable system, Anal. Biochem. 130 (1983) 134–145.
[19] P.F. Davison, Proteins in denaturing solvents: gel exclusion studies, Science 161 (1968) 906–907.
[20] N. Sreerama, R.W. Woody, A self-consistent method for the analysis of protein secondary structure from circular dichroism, Anal. Biochem. 209 (1993) 32–44.
[21] M.R. Eftink, Use of multiple spectroscopic methods to monitor equilibrium unfolding of proteins, Methods Enzymol. 259 (1995) 487–512.
[22] J.J. Pan, S.T. Chiu, P.H. Liang, Product distribution and pre-steady-state kinetic analysis of *E. coli* undecaprenyl pyrophosphate synthase, Biochemistry 39 (2000) 10936–10942.
[23] J.J. Pan, L.W. Yang, P.H. Liang, Effect of site-directed mutagenesis of the conserved aspartate and glutamate on *E. coli* undecaprenyl pyrophosphate synthase catalysis, Biochemistry 39 (2000) 13856–13861.
[24] T.P. Ko, Y.K. Chen, H. Robinson, P.C. Tsai, Y.G. Gao, A.P.-C. Chen, A.H.-J. Wang, P.H. Liang, Mechanism of the product chain length determination and the role of a flexible loop in undecaprenyl pyrophosphate synthase catalysis, J. Biol. Chem. 276 (2001) 47474–47486.
[25] T. Kainou, K. Okada, K. Suzuki, T. Nakagawa, H. Matsuda, M. Kawamukai, Dimer formation of octaprenyl-diphosphate synthase (*IspB*) is essential for chain length determination of ubiquinone, J. Biol. Chem. 276 (2001) 7876–7883.
[26] S.F. Altschul, T.L. Madden, A.A. Schaffer, J. Zhang, Z. Zhang, W. Miller, D.J. Lipman, Gapped BLAST and PSI-BLAST: a new gener-

ation of protein database search program, Nucleic Acids Res. 25 (1997) 3389–3402.
[27] B. Soballe, R.K. Poole, Microbial ubiquinones: multiple roles in respiration, gene regulation and oxidative stress management, Microbiology 145 (1999) 1817–1830.
[28] Y.H. Chen, A.P.-C. Chen, C.T. Chen, A.H.-J. Wang, P.H. Liang, Probing the conformational change of *Escherichia coli* undecaprenyl pyrophosphate synthase during catalysis using an inhibitor and tryptophan mutants, J. Biol. Chem. 277 (2002) 7369–7376.